New Journal of Physics
The open access journal at the forefront of physics

Deutsche Physikalische Gesellschaft DPG IOP Institute of Physics

PAPER • OPEN ACCESS

# Control of mobile chaotic agents with jump-based connection adaption strategy

To cite this article: Jie Zhou *et al* 2020 *New J. Phys.* **22** 073032

New Journal of Physics
The open access journal at the forefront of physics

Deutsche Physikalische Gesellschaft DPG
IOP Institute of Physics

Published in partnership with: Deutsche Physikalische Gesellschaft and the Institute of Physics

OPEN ACCESS

RECEIVED
23 March 2020

REVISED
16 May 2020

ACCEPTED FOR PUBLICATION
1 June 2020

PUBLISHED
22 July 2020



PAPER

# Control of mobile chaotic agents with jump-based connection adaption strategy

**Jie Zhou**[1,2], **Yinzuo Zhou**[3,5], **Gaoxi Xiao**[4] and **H Eugene Stanley**[2]

[1] School of Physics and Electronic Science, East China Normal University, Shanghai 200241, People's Republic of China
[2] Center for Polymer Studies and Department of Physics, Boston University, Boston, MA, 02215, United States of America
[3] Alibaba Research Center for Complexity Sciences, Hangzhou Normal University, Hangzhou 311121, People's Republic of China
[4] School of Electrical and Electronic Engineering, Nanyang Technological University, Singapore 639798
[5] Author to whom any correspondence should be addressed.

**E-mail:** zhouyinzuo@163.com

**Keywords:** connection adaption strategy, synchronization control, mobile agents

## Abstract

The connection adaption strategy (CAS) has been proposed for the synchronization of networked mobile chaotic agents, which is considered to be a simpler scheme compared to commonly used coupling adaption strategies. However, this strategy only provides a limited range of feasible coupling strength allowing a success control. In this paper, we develop the CAS by introducing a jump process to resolve this problem. We show that the proposed approach systematically outperforms the original CAS in the whole range of the mobility and the range of feasible coupling strength is extensively expanded. In addition, we show that motion of the agents could be classified into three different regimes. The dynamical features of these motion regimes are analyzed and relevant measures are provided to characterize the controllability of the network in each regime.

## 1. Introduction

Synchronization is one of the most important cooperative dynamics that is widely observed in different disciplines [1–4]. In many circumstances, synchronization is a useful behavior that may bring valuable outcomes to the systems, such as power grid network [5], moving robots networks [6, 7], and physiological networks in biological systems [8–10]. Vast amount of efforts have been devoted to induce the dynamics of elements in systems toward the desired common states. Along with the developments of studies on complex networks, various control strategies have been proposed for synchronization of network systems [11–14], making it a central topic of network theory.

Traditional studies on complex networks are typically under the limiting assumptions of quenched and annealed networks [15, 16], where the time scale of network structure evolution is either much slower or much faster than that of the nodal dynamical process. Recently, increasing attentions have been focusing on more general situations where the two time scales are comparable [17–20]. The studies on synchronization control have also been following this direction and many results have been obtained under the framework of temporal networks [21–28].

For existing studies about synchronization in temporal networks, a common approach is to consider the systems where mobile agents carry oscillatory dynamics and perform random walk in a certain space [29–31]. A majority of investigations of synchronization control on temporal networks are based on this framework or similar variations [30–32]. With limited knowledge of randomly varying structure, adaptive control strategies become a favorable choice for this kind of networks [33–37]. However, these strategies are mainly performed under the theme of adaptively adjusting the coupling strength between agents, here referred as coupling adaption strategy.

Recently, a strategy, referred as connection adaption strategy (CAS), has been proposed where agents only need to activate or deactivate the connection with their neighbors [38]. An important advantage of the CAS is that it may be simpler to be implemented than coupling adaption strategies do, since treating

coupling in an on–off manner will certainly be more convenient than in an continuous manner, making the CAS be a promising scheme for synchronization control. This on–off simplicity endows the CAS great application potential, as many empirical networks contain the on–off feature in their time-varying structure [39, 40]. However, it has also been shown that in CAS an agent sometimes cannot find a proper neighbor to establish a connection which may damage the effectiveness of the strategy. Though few remedies have been proposed to relief this situation [38, 41], limitation in the effect of the strategy is still imposed, reflected by a relative small range of feasible coupling strength for a successful control. Therefore, an approach that may release this restriction is still in demand.

In this work, we consider an alternative approach to tackle this problem. We introduce a jump process for agents to find proper neighbors in the case when there is no suitable neighbor around. This jump process could be taken as a simplified approximation of a long distance walk in a short time [28], which has been observed in some social systems [42] biological systems [43] and robotic systems [44]. We show that this proposed approach systematically outperforms the original CAS [38]. In addition, we systematically investigate the effect of the approach on the whole speed range, finding that the whole range could be divided into three regimes. For each regime a proper measure is introduced to predict the controllability of the network, which is well matched with simulation results.

## 2. Model

We consider a unit planar space $\Gamma$ with length $L$, where an ensemble of $N$ mobile agents move freely in it with periodic boundary conditions. The velocity of an arbitrary agent $i$ is $\mathbf{v}_i(t) = (v\cos\theta_i, v\sin\theta_i)$, where the speed $v$ is the same for all the agents and the direction $\theta_i$ is randomly drawn from the interval $[-\pi, \pi)$ with uniform probability (at each time step). Therefore, the position of agent $i$, $y_i(t)$, updates as $y_i(t+\Delta t) = y_i(t) + v_i(t)\Delta t$, where $\Delta t$ is the length of a time step.

All agents carry an identical chaotic dynamics described by $\dot{\mathbf{x}}^i(t) = \mathbf{F}(\mathbf{x}^i)$ with $\mathbf{x}^i \in \mathbf{R}^m$, $i = 1, 2, \ldots, N$, dot denotes temporal derivative, and $\mathbf{F}: \mathbf{R}^m \to \mathbf{R}^m$. All agents have identical contact radius $r$, and when any pairs of them are within the radius of each other, a temporal connection may be built depended on states and position information of them. The temporal interacting structure could be described by a Laplacian matrix $G(t)$ where an un-weighted element $g_{ij}(t) = -1$ indicates that agent $i$ forms a directed connection with agent $j$ and $g_{ij}(t) = 0$ otherwise. The diagonal elements $g_{ii}(t) = -\sum_{j\neq i} g_{ij}(t)$ warrant the zero-row-sum property of $G(t)$. With the interaction with other agents, the dynamics of each agent $i$ is governed by

$$\dot{\mathbf{x}}^i(t) = \mathbf{F}(\mathbf{x}^i) - \sigma\sum_{j=1}^{N} g_{ij}(t)\mathbf{H}(\mathbf{x}^j), \tag{1}$$

where $\sigma$ is the coupling strength and $\mathbf{H}: \mathbf{R}^m \to \mathbf{R}^m$ is a coupling function defining how a connected neighbor impacts.

In this work, our purpose is to control the agents toward a desired solution $\mathbf{x}^1 = \mathbf{x}^2 = \cdots = \mathbf{x}^N = \mathbf{x}^S$. To this aim, one or several units that carry the target solution $\mathbf{x}^S$ is necessary to be deployed in the network for other agents to follow, i.e. pinning synchronization control. We follow the spirit of connection adaption strategy (CAS) where agents may adaptively rewire connections with their neighbors under a prescribed rule. The key procedure of CAS is as follows. First placing a unit which carries the target solution at an arbitrary position of the space $\Gamma$. This unit is fixed on the position and this position is known to all the agents. It could be regarded as a virtual agent and we refer to it as the guide agent (GA). Then, the agents will adaptively establish connections with neighbors by the rules that, at each time step, an agent $i$ attempts to choose one of its neighbors, say agent $j$, to form up a direct connection (so that $g_{ij}(t) = -1$). However, this agent $j$ should satisfy two conditions: (i) it is the one nearest (among all neighbors of agent $i$ within a disk of radius $r$) to the GA (if the GA is a neighbor of agent $i$, GA itself will be chosen); (ii) the distance between the connected agent and the GA is smaller than that between agent $i$ and the GA. If all the agents successfully find suitable neighbors for connection, an acyclic structure will be formed with directed connections uniformly pointing from the periphery to the GA, giving a lower triangular Laplacian matrix $G(t)$ as follows

$$G(t) = \begin{pmatrix} 0 & & & \\ & 1 & & 0 \\ & & \ddots & \\ 0 \text{ or } -1 & & & 1 \end{pmatrix}, \tag{2}$$

with proper relabeling of the agents' indexes (GA is indexed 1 all the time), where $g_{ii} = 0$, $g_{ii} = 1 (i \neq 1)$, $g_{ij(i<j)} = 0$, and $g_{ij(i>j)} = 0$ or $-1$. The spectrum of $G(t)$ is $\lambda_1 = 0$ (corresponding to the synchronization

manifold $\mathbf{x}^{\mathrm{S}}$) and $\lambda_2 = \cdots = \lambda_{N+1} = 1$ (corresponding to the transverse modes). Since the eigenvalues of the transverse modes are all the same, giving $\lambda_2/\lambda_{N+1} = 1$, the resulting structure is an optimal one favoring a stable synchronization [14, 45]. Specifically, the condition $\lambda_2 = \cdots = \lambda_{N+1} = 1$ gives an identical variational equation for all the $N$ transversal modes as follows

$$\dot{\zeta} = [D\mathbf{F} + \sigma D\mathbf{H}]\zeta, \tag{3}$$

where $D\mathbf{F}$ and $D\mathbf{H}$ are the Jacobian functions of $\mathbf{F}$ and $\mathbf{H}$, respectively. The maximum transversal Lyapunov exponent could then be obtained from equation (3) as a function of coupling $\sigma$, and we refer to this exponent function as master stability function (MSF) $\Phi(\sigma)$. According to the MSF theory [46], the necessary condition of obtaining a stable synchronization of the network is $\Phi(\sigma) < 0$.

However, when the density of the agents is not high enough, it is likely that some agents may not be able to find suitable ones to follow. When such an event happens, in CAS an agent may temporarily expand its contact radius until a qualified agent is reached. This remedy may, however, cause a strong restriction that for those agents whose topological distance (number of hops) is larger than a critical distance they cannot be synchronized. As indicated in figure 1(b), for systems with agents having large topological distance the feasible coupling strength for a successful control may be squeezed in a narrow range, unfavorable for control. Here, we address this issue by proposing an alternative scheme that when such event happens on an agent, this agent will perform a random jump in the space $\Gamma$ for searching other suitable agents. The jump process continuous until a proper agent is found; after that the agent will resume to the normal state with a speed $v$. To distinct from the CAS, we refer to this jump-based CAS as JCAS.

For the sake of illustration, we endow the agents with chaotic Rössler oscillator. The dynamics of each unit is described by $\dot{x}_1^i = -(x_2^i + x_3^i)$, $\dot{x}_2^i = \dot{x}_1^i + a\dot{x}_2^i$, $\dot{x}_3^i = b + x_3^i(x_1^i - c)$, where $\mathbf{x}^i = (x_1^i, x_2^i, x_3^i)^{\mathrm{T}}$ and $a = b = 0.2$, $c = 5.7$. $\mathbf{H}(\mathbf{x}) = (x_1, 0, 0)$ realizes a linear coupling on the $x_1$ variable of the units. The dynamics is integrated with a fixed integration time step $\Delta t = 0.001$. The master stability function $\Phi(\sigma)$ could thus be calculated by inputting these conditions into equation (3). In the simulation, without loss of generality the network size is set $N = 100$ and the contact radius $r = 0.1$ unless specified otherwise. The error function $\delta_i = 1/3(|x_1^i - x_1^1| + |x_2^i - x_2^1| + |x_3^i - x_3^1|)$ is monitored to evaluate the control performance on unit $i$. $\delta(t) = 1/N\sum_{i=2}^{N+1}\delta_i(t)$ (the average error of all the units) and $\langle\delta\rangle$ (the time-averaged value of $\delta(t)$ over the last $10^6$ integration time steps) are evaluated after a suitable transient time, to characterize the global control performance. We note that since in this case all the agents share an identical Rössler dynamics, the evaluation that whether the network is fully synchronized could be implemented by checking whether $\langle\delta\rangle \to 0$. However, for more complicated cases that oscillators may have parameter/frequency mismatch where a full synchronization is hard to reach, a pre-processing technique, e.g. utilizing a bandpass filter [47], may be used to the output signals of the oscillators so as to characterize different extent of the synchronization of the network. In this paper, all the simulation results are performed under 100 different realizations and error-bars in the figures stand for standard deviation.

## 3. Results

### 3.1. The case of $v = 0$

Let us start from the simple case of $v = 0$. In this case, all the agents are fixed on their respective locations in the space $\Gamma$. Thus, for randomly distributed initial positions, some agents may not have proper neighbors to establish connections following the rule of CAS. For this case, these agents will perform random jump as suggested by JCAS (as contrast to the strategy of expanding their contact radius in CAS) until suitable candidates are found. When all the agents have found proper ones for connection, they will stay on their new locations from then on and the resulting structure will be a static tree with directed edges pointing from peripheral to the GA. We compare the performance of JCAS and CAS for the case of $v = 0$ in figure 1(a). We can see in both schemes, the network can be controlled ($\langle\delta\rangle \to 0$) in the range about $0.2 < \sigma < 2.8$, indicating similar effects in this specific case.

As pointed, when $v = 0$ the resulting structures of both schemes are directed trees uniformly pointing from periphery to the GA. This kind of tree structures could be regarded as a group of uni-directional chains ending at the GA [see the example in the bottom in figure 1(b)] and overlapped at some sections. It can be found that the spectrum of such an uni-directional chain is $\lambda_1 = 0$ and $\lambda_{i\geqslant 2} = 1$. For Rössler system, $\Phi(\sigma) < 0$ when $\sigma \in (\sigma_1, \sigma_2)$ with $\sigma_1 \simeq 0.13$ and $\sigma_2 \simeq 4.25$ [see figure 1(c)], defining an optimal range of the coupling strength $\sigma$ allowing a successful control. On the other hand, the actual range of $\sigma \in (0.2, 2.8)$ shown in figure 1(a) allowing a successful control is apparently smaller than the optimal range $(\sigma_1, \sigma_2)$, which suggests the existence of other factors playing a crucial role to the performance of the approach. For a structure as simple as an uni-directional chain, the only factor related to the structure is the length of the

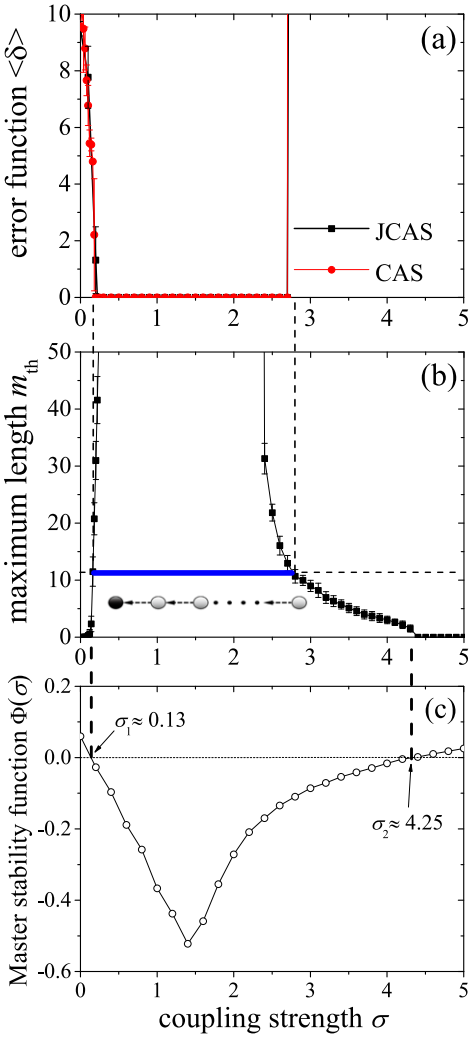


**Figure 1.** The performances of JCAS (black curves) and CAS (red curves) for the case of $v = 0$ are presented with the behaviors of $\langle\delta\rangle > 0$ with $N = 100$ and $r = 0.1$. The black and red curves almost collapse on each other. (b) Relation between the coupling strength $\sigma$ and the maximum length of an uni-directional chain $m_{\text{th}}$ permitting synchronization. The blue line indicates the range of $\sigma$ allowing synchronization where the $m_{\text{th}}$ equals 11. The vertical dashed line between (a) and (b) denote the accordance of the range of allowable $\sigma$. The chain at the bottom of (b) is an example of uni-directional chain, where the black circle represents the GA and gray circles represent the agents on the chain for synchronization. (c) The master stability function of Rössler system $\Phi(\sigma)$. The range of $\sigma$ for $\Phi(\sigma) < 0$ confines the possible range of $\sigma$ for synchronization. The vertical dashed lines connect panels (b) and (c) indicate the accordance between the boundaries of $\Phi(\sigma)$ and positive $m_{\text{th}}$ where a synchronization is possible.

chain. This speculation is verified in figure 1(b), where every given coupling strength $\sigma$ corresponds to an upper bound of the length of the chain $m_{\text{th}}$, allowing a stable synchronization. This result also tells that a longer uni-directional chain is more difficult to be synchronized. Since the synchronization of the whole network needs to have all the chains to be synchronized, the controllability is therefore determined by the longest chain in the network. Defining the topological distance (TD) between an agent and the GA as the distance between them on an uni-directional chain, the controllability of the network is thus determined by the largest TD. The blue line in figure 1(b) indicates $m_{\text{th}} \simeq 11$ when $\sigma = 2.8$, and this distance is well matched with the length of the longest chains obtained from JCAS and CAS, confirming the key role of the length of the uni-directional chain for a synchronization control.

### 3.2. The case of $v \neq 0$

When $v \neq 0$, the agents will move freely on the square and a tree structure could be broken and reformed intermittently. Thus, the longest TD defined in the static case may be no longer valid to indicate the controllability of network, which demands new measures to evaluate this more complicated situation. We first examine the performance of the JCAS and CAS for different speed values $v$ as shown in figures 2(a)–(c). For $v = 1$, the performance of JCAS is slightly improved as reflected by a small increment in the right boundary of feasible coupling strength $\sigma$, which is denoted as $\sigma_{\text{th}}$. For $v = 10$, the performance of JCAS is evidently improved and $\sigma_{\text{th}}$ is close to the optimal boundary $\sigma_2 \simeq 4.25$ in the static case. For

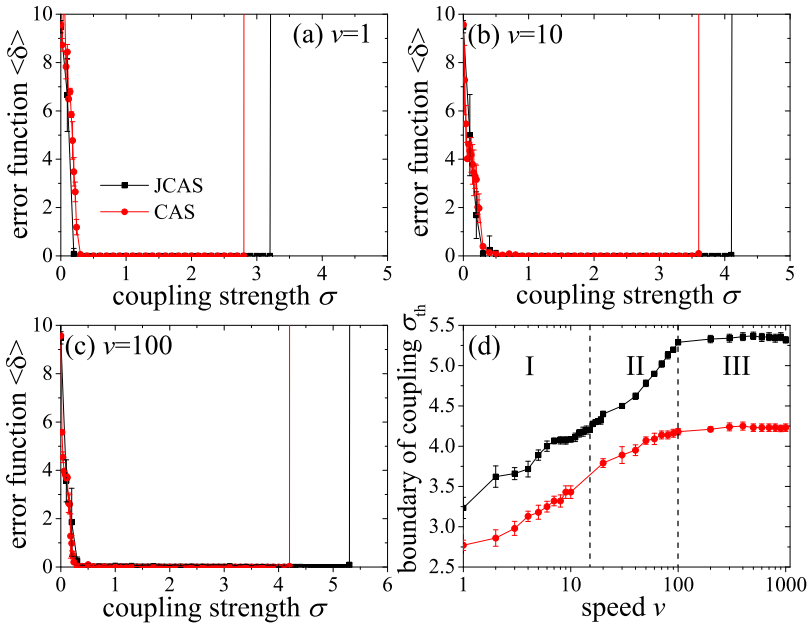


**Figure 2.** Performances of JCAS (black curves) and CAS (red curves) for (a) $v = 1$, (b) $v = 10$, and (c) $v = 100$. When $\langle\delta\rangle \to 0$ ($\langle\delta\rangle > 0$), all the agents in the network are (are not) synchronized. (d) The right boundary of coupling strength allowable for synchronization, $\sigma_{\rm th}$, as functions of speed $v$ for JCAS and CAS. A larger value of $\sigma_{\rm th}$ indicates a wider range of feasible coupling strength for synchronization. For JCAS (black curve), the range of speed $v$ is separated into three regimes as indicated by two vertical dashed lines. The dashed line separating regimes I and II happens at $\sigma_{\rm th} = \sigma_2 \simeq 4.25$, and the dashed line separating regimes II and III happens at $v_{\rm th} \simeq r/\Delta t = 100$. Other parameters are the same as those in figure 1.

$v = 100$, the feasible range of JCAS is remarkably expanded where $\sigma_{\rm th} \simeq 5.4$ is even beyond the boundary $\sigma_2$. On the other hand, in all these cases, the performances of JCAS evidently outperforms CAS with a much wider range of feasible coupling strength. Figure 2(d) shows the behavior of $\sigma_{\rm th}$ both for JCAS and CAS on the full range of speed $v$. As a larger $\sigma_{\rm th}$ corresponds to a larger allowable range of coupling strength for synchronization control, it is clear that the performance of JCAS is systematically superior to that of CAS in the whole motion range.

Furthermore, the results in figure 2(d) suggests that the motion speed $v$ could be separated into three characteristic regimes, which are: regime I ($1 \leqslant v \leqslant 15$) where $\sigma_{\rm th}$ grows fast and saturate at around $\sigma_2 \simeq 4.25$; regime II ($15 < v < 100$) where $\sigma_{\rm th}$ grows from 4.25 to about 5.4; and regime III ($v > 100$) where $\sigma_{\rm th}$ stables at about 5.4. In the following, we will analyze the behaviors of $\sigma_{\rm th}$ in the three regimes, respectively, to understand the mechanism of JCAS under different speed motions.

**Regime I**. In this regime, the speed $v$ is relative small. Thus, when an agent $i$ follows another agent, say $j$, with a direct connection, this connection may be kept for a relative long time since agent $i$ may linger around $j$ for quite a while. On the other hand, though agent $i$ move slowly, it will eventually move far enough from $j$ and then the connection breaks. When such event happens and meanwhile there is no other valid neighbor for connection, agent $i$ will perform a random jump to search for new candidate for connection under the rule of JCAS. In fact, this process is equivalent to break an uni-directional chain and then form a new one. As a result, the largest TD (one of the key factors for synchronization for a static structure) between agents and the GA will be reduced, since it is very unlikely that an agent is always the furthest one when a chain is reshuffled. To quantitatively measure this effect, we introduce a quantity named effective distance of agent $i$ as $\overline{m}_i$ to characterize the temporal TD between $i$ and the GA. Specifically, suppose in a long enough period of time in which there are $M$ time steps that agent $i$ could reach the GA through a pathway (while in the rest time steps agent $i$ fails to reach the GA), and the TD of the $M$ steps are $m_i(1), m_i(2), \ldots, m_i(M)$, respectively. Then, $\overline{m}_i$ is defined as the average of these TDs, i.e. $\overline{m}_i = 1/M\sum_{k=1}^{M} m_i(k)$. Furthermore, we denote $\overline{m}_{\rm max} = \max\{\overline{m}_i; \forall i\}$ as the largest effective distance among all the agents. Obviously, in the case of $v = 0$, $\overline{m}_{\rm max}$ equals the largest TD, while when $v$ increases, $\overline{m}_{\rm max}$ is expected to decrease. The behavior of $\overline{m}_{\rm max}$ shown in figure 3(a) validates this expectation. Combining the $v$–$\sigma_{\rm th}$ relation in figure 2(d) and $v$–$\overline{m}_{\rm max}$ relation in figure 3(a) interprets the $\sigma_{\rm th}$–$\overline{m}_{\rm max}$ relation. The relations $\sigma_{\rm th}$–$\overline{m}_{\rm max}$ and $\sigma$–$m_{\rm th}$ are presented together in figure 3(b), and the overlapping of the two curves indicates that the $\overline{m}_{\rm max}$ is a proper factor to determine the controllability of JCAS in regime I as $m_{\rm th}$ does in the static case.

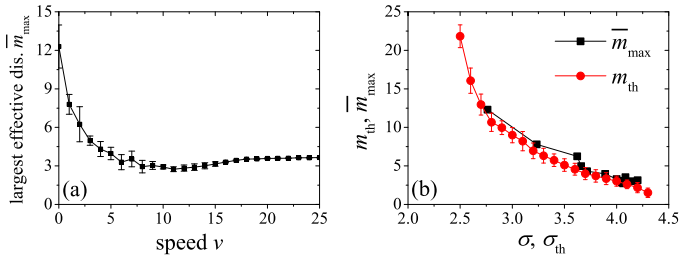


**Figure 3.** (a) The behavior of the largest effective distance $\overline{m}_{max}$ as a function of speed $v$ for $r = 0.1$. (b) Comparison between the $\sigma$–$m_{th}$ relation of uni-directional chain and the $\sigma_{th}$–$\overline{m}_{max}$ relation derived from the $v$–$\overline{m}_{max}$ and the $v$–$\sigma_{th}$ relations for the case of $v \neq 0$.

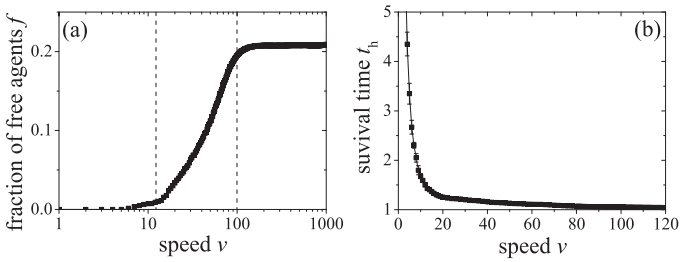


**Figure 4.** Behaviors of (a) $f$, indicating the possibility that an agent fail to find suitable neighbors for connection in a time step, saturates around $f_{th}$ when $v > 100$, and (b) average survival time of temporal connections $t_h$, as a function of $v$.

We remark that in a certain time step an agent may have a possibility that it fails to find a suitable neighbor to follow. This possibility is equivalent to the fraction of such agents in a time step averaged over a long period of time. For convenience, we denote such agent as freely evolving agent and the corresponding possibility of such event to happen as $f$. It can be understood that in regime I, so that the motion is slow, $f$ could be very small [see figure 4(a)] which means an agent $i$ may have valid TDs in most time steps, thus the introduced $\overline{m}_i$ could be a relevant parameter to reflect the topological relation between it and GA. However, when the speed $v$ further grows into regimes II and III, the possibility $f$ shall also increase, and a connection is more likely to be broken which may lead the indicator $\overline{m}_{max}$ to be deviated from and invalid to describe the actual situation.

**Regime III**. Now, we turn to the case of regime III, where the speed $v > 100$ is fast. With the setting $r = 0.1$, $\Delta t = 10^{-3}$ and defining $v_{th} = r/\Delta t = 100$, in this regime, an agent will almost certainly separate from the followed agent in one time step because of $v > v_{th}$. Thus, in this regime almost all the connections are broken and new connections are formed consistently. This occasion actually makes the network act as a fast-varying network. For a fast-varying network, it has been proved that the condition to maintain a stable synchronization is equivalent to that of a static network which structure is the aggregation of the varying structures of the original temporal networks [48]. Therefore, to evaluate the stability of a synchronization in regime III could be transformed to the problem of evaluation on its corresponding aggregated network.

The structure of the aggregated network can be calculated with the following facts. First, as defined in the JCAS, when an agent is in the disk of radius $r$ centered at the GA, it will definitely follow the GA. Therefore, in each time step an agent has a possibility of $b = \pi r^2/L^2$ to follow the GA directly. Secondly, since an agent has a possibility $f$ to freely evolve (failed to find a proper neighbor to connect) in a time step, the possibility of it following the rest $N-1$ agents (except for itself and GA) equals $1-f-b$. As these $N-1$ agents are equal footing, the possibility for each of them to be followed by the agent then equals $(1-f-b)/(N-1)$. These facts draw us to the Laplacian matrix $\overline{G}$ of the aggregation network as

$$\begin{pmatrix} 0 & \cdots & \cdots & \cdots & 0 \\ -b & 1-f & -\frac{1-f-b}{N-1} & \cdots & -\frac{1-f-b}{N-1} \\ \vdots & -\frac{1-f-b}{N-1} & 1-f & \ddots & \vdots \\ \vdots & \vdots & \ddots & \ddots & -\frac{1-f-b}{N-1} \\ -b & -\frac{1-f-b}{N-1} & \cdots & -\frac{1-f-b}{N-1} & 1-f \end{pmatrix}_{(N+1)\times(N+1)}, \tag{4}$$

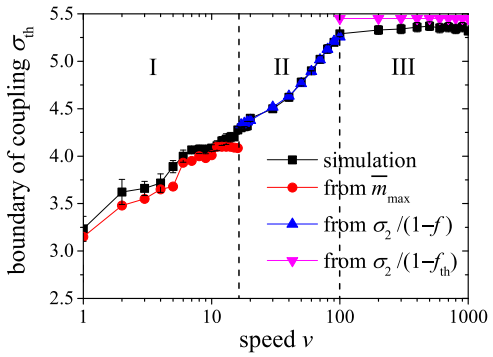


**Figure 5.** Comparisons for the $v$–$\sigma_{th}$ relation between the simulation results (black curves) and different measurements for the three regimes, respectively.

where $\overline{G}_{11} = 0$ (GA is always indexed as 1), $\overline{G}_{1i} = 0$ ($I \geqslant 2$), $\overline{G}_{i1} = -b$ ($i \geqslant 2$), $\overline{G}_{ii} = 1 - f$ ($i \geqslant 2$), $\overline{G}_{i\neq j} = -\frac{1-f-b}{N-1}$ ($i \geqslant 2, j \geqslant 2$). Solving the spectrum of $\overline{G}$, one gets $\lambda_1 = 0$ and $\lambda_2 = \cdots = \lambda_{N+1} = 1 - f$. For this specific case, where connections are consistently broken and agents apply the jump process almost all the time, we denote the possibility that an agent is freely evolving in a time step as $f_{th}$. The value of $f_{th}$ could be well estimated (details are provided in the appendix A), and in the setting of $N = 100$ and $r = 0.1$, we have $f_{th} \approx 0.22$ which is validated by the results in figure 4(a). Now, since the eigenvalue of the transversal modes of the aggregated network is $1 - f_{th}$ and the condition for a stable synchronization is $\Phi(\sigma\lambda) < 0$, the boundary of the coupling strength $\sigma_{th}$ should satisfy $\sigma_{th}(1 - f) = \sigma_2$. Inputting $\sigma_2 \simeq 4.25$ and $f_{th} \approx 0.22$, we get $\sigma_{th} \approx 5.45$. This analytical estimation exhibits good accordance with the simulation results as shown in figure 5, verifying the fast-varying feature of the network in this regime.

**Regime II**. Now, we come to the case of regime II. As shown in figure 2(d), in this regime, $\sigma_{th}$ grows gradually with the increasing of $v$. To better understand this behavior, we take detail observations on the structural property of temporal networks. First, we measure the average survival time of temporal directed connections between agents, which is denoted as $t_h$. The behavior of $t_h$ as a function of $v$ is presented in figure 4(b). We can see that it decreases rapidly as the increasing of $v$ in regime I ($t_h \to \infty$ when $v = 0$). In the regimes of II and III, i.e. when $v > 15$, we observe $t_h < 1.25$, which manifests that a connection is not likely to persist in two consecutive time steps in these regimes. This observation strongly suggests that in regime II the temporal network is also fast-varying.

However, the $v$–$f$ relation shown in figure 4(a) tells that in the regime II the fraction $f$ is smaller than that in the region III. This is due to the fact that an agent with a smaller $v$ may follow its neighbor with more consecutive time steps as it may take a longer time to move far enough to break the connection. On the other hand, if an agent is not following anyone else, the possibility of it finding a proper agent for connection through the jump process is independent of the motion speed. Combining these two effects results in a lower possibility $f$ with a smaller $v$. Thus, the above observations clearly illustrate that networks in the regime II should still be fast-varying but with a smaller possibility $f$ than that in regime III. Hence, the relation $\sigma_{th} = \sigma_2/(1 - f)$ is still valid in this regime. By imposing the value of $f$ for different $v$ in regime II collected from figure 4(a), we obtain the estimated value of $\sigma_{th}$ in the regime II as illustrated in figure 5. We can see that this prediction well matches the simulation results.

### 3.3. The impact of radius *r*

Finally, we examine the effect of JCAS on different contact radius $r$. We first present the $v$–$\overline{m}_{max}$ relation of $r = 0.04$, 0.06, 0.08, and 0.1 for slow motion regime (regime I) in figure 6(a). One can see that all these curves converge to about 2.7, but the curve for a smaller $r$ converges faster. In fact, for a smaller $r$, a connection is easier to break since a follower is easier to leave the $r$-disk of the followed agent. Actually, the rate to leave the disk is proportional to $v/r$, and therefore inversely proportional to the characteristic time that a connection could preserve. This argument is validated by the rescaled plot in the inset of figure 6(a) where the rescaled behaviors overlap. Then, for fast motion regime (regimes II and III), we show the $v$–$f$ relation for the same set of $r$ values in figure 6(b). We observe that the behavior of these curves share similar tendency. Moreover, as to the $v$–$f$ relation, besides the rescaling $v \to v/r$, the possibility $f$ is also influenced by $r$ which is encoded in the relation between $r$ and $f_{th}$ (see appendix A). By imposing the rescaling of $v \to v/r$ and $f \to f_{th}$, the rescaled behaviors of $v$–$f$ relation are shown in the inset of figure 6(b). We can see that these curves largely conform, revealing the impact of $r$ on $f$ to the performance in these regimes. Further, we present the behaviors of $\sigma_{th}$ as functions of $v$ for the same set of $r$ values in figure 6(c). As

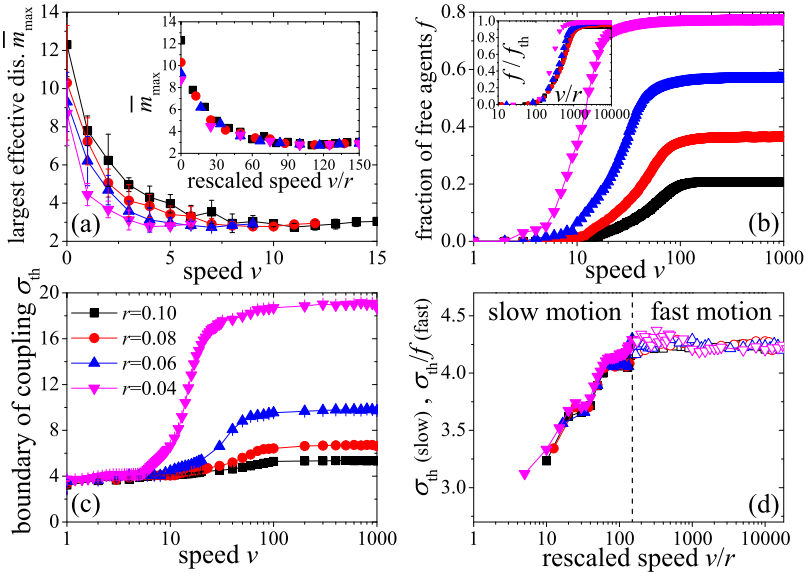


**Figure 6.** Behaviors of (a) $v$–$\overline{m}_{max}$, (b) $v$–$f$, and (c) $v$–$\sigma_{th}$ relations for the case of $r = 0.10$ (black), $r = 0.08$ (red), $r = 0.06$ (blue), and $r = 0.04$ (magenta), respectively. The inset of panel (a) is a rescaled plot of (a) with $v \to v/r$. The inset of panel (b) is a rescaled plot of (b) with $v \to v/r$ and $f \to f/f_{th}$. (d) A rescaled plot of (c) with $v \to v/r$ and $\sigma_{th} \to \sigma_{th}$ (slow motion) or $\sigma_{th} \to \sigma_{th}(1-f)$ (fast motion). The dashed line separates the two speed motions where $\sigma_{th}$ reaches $\sigma_2 \simeq 4.25$.

suggested by the scaling properties in figures 6(a) and (b), the $v$–$\sigma_{th}$ relation should also satisfy similar scaling features. To show this, for each radius $r$, we separate the speed into slow motion and fast motion with the condition of $\sigma_{th} = \sigma_2$ separating the regimes I and II and the condition of $v_{th} = r/\Delta t$ separating the regimes II and III. Then, we rescale the slow motion with $v \to v/r$ and fast motion with $v \to v/r$ and $\sigma_{th} \to \sigma_{th}(1-f)$. Resulting behaviors are presented in figure 6(d). Clearly, the overlapping of these rescaled behaviors under different radius $r$ proves the above conditions classifying the regimes and the effectiveness of related measures.

## 4. Conclusion

In summary, we have developed the connection adaption strategy (CAS) by introducing a jump process for the purpose of synchronization control of networks with mobile chaotic agents. The jump process is exerted when an agent cannot find a proper neighbor to apply the CAS. Our results have shown that the effect of jump-based CAS (JCAS) completely outperforms the original CAS. In addition, we have found three different dynamical regimes in JCAS. In the regime where agents move slowly, the network in each time step could be characterized by a group of uni-directional chains pointing to the guide agent (GA) which carries the target synchronization solution. A measure, referred as the largest topological distance, is introduced to describe the temporal distance between agents and the GA, which is shown to be a good estimator to predict the controllability of the system in this regime. In the other limit, where agents move very fast, the relations between each pair of agents may change in almost every time step, and the structures between two consecutive time steps are largely independent. By analytically calculating the fraction of freely evolving agents, which temporally fail to find proper neighbors for connection, the range of coupling strength permitting successful control is well predicted. For the medium regime of motion speed, we have found that the network could also be regarded as fast-varying networks. However, in this regime the fraction of freely evolving agents varies with the motion speed. We have shown that this fraction grows gradually with the increasing of the speed, and the range of feasible coupling strength expands from low speed regime to high speed regime.

For the topic of controlling dynamical systems where individual units could move freely in a space, CAS may have advantage for easier implementation than traditional coupling adaptive strategies. The jump-based method proposed in this paper could effectively enhance the effectiveness of the CAS. The primary role of our work is to emphasize the potential of the CAS scheme. In the current setting, the jump process can be regarded as a high speed movement. However, this process may be generalized by dealing with the speed of freely evolving agents in a delicate manner applied to more realistic scenarios. As new network perspectives of dynamical systems with varying structures are continuously emerging in theoretical

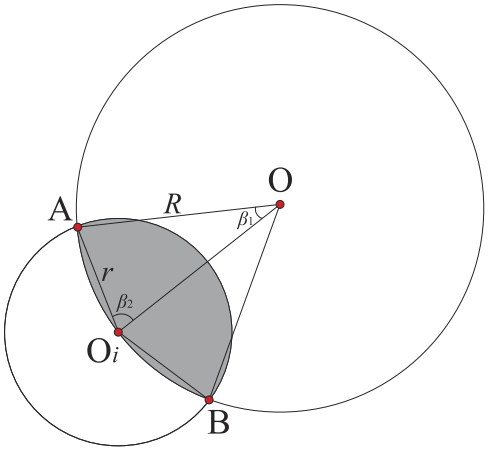


**Figure A1.** Diagram for the evaluation of possibility $f_{\text{th}}$. The GA is located at the center of the plane $O$. Agent $i$ is located at $O_i$ which is at a distance $R$ to the $O$. The two circles (the big one centered at $O$ with radius $R$ and the small one centered at $O_i$ with radius $r$) intersects at A and B, and overlap in the shaded area. $\beta_1$ and $\beta_2$ represent the radians of angle $\angle AOO_i$ and $\angle AO_iO$, respectively.

and empirical context [49, 50], further exploitation of the CAS applying to these systems is of future research interest.

## Acknowledgments

This work was supported in part by the National Natural Science Foundation of China under Grant 11835003, in part by the Ministry of Education, Singapore, under Contract MOE2016-T2-1-119, and in part by NSF Grant PHY-1505000 and by DTRA Grant HDTRA1-14-1-0017.

## Appendix A. Evaluation of $f_{\text{th}}$

In this appendix, we derive the possibility $f_{\text{th}}$ that in a time step an agent has no suitable neighbor for connection when agents continuously jump.

Suppose an agent $i$ located at $O_i$ is at a distance $R$ to the GA located at the center of the plane $O$ (see figure A1). As defined in the JCAS, if agent $i$ has no suitable neighbor for connection, it means that in the sub-area, which is the overlap between the $r$-disk centered at $O_i$ and $R$-disk centered at $O$ (shaded region in figure A1), there is no agent inside it (otherwise a feasible connection is available to agent $i$). To calculate the possibility that an agent has no neighbor for connection, we first calculate the area of this shaded region, denoted as $S$.

It can be seen that the size of the area $S$ satisfies $S = S_{\widehat{AOB}} + S_{\widehat{AO_iB}} - 2S_{\Delta AOO_i}$, where $S_{\widehat{AOB}}$ and $S_{\widehat{AO_iB}}$ are the areas of sectors $\widehat{AOB}$ and $\widehat{AO_iB}$, respectively, and $S_{\Delta AOO_i}$ is the area of the triangle $\Delta AOO_i$. We assume the radian of the angles $\angle AOO_i$ and $\angle AO_iO$ are $\beta_1$ and $\beta_2$, respectively, then we have $S_{\widehat{AOB}} = 2\beta_1/2\pi \cdot \pi R^2$ and $S_{\widehat{AO_iB}} = 2\beta_2/2\pi \cdot \pi r^2$. The $S_{\Delta AOO_i}$ could be calculated with Heron's formula which gives

$$\begin{aligned} S_{\Delta AOO_i} &= 1/4\sqrt{(2R+r)(2R-r)(R+r-R)(R+r-R)} \\ &= r/4\sqrt{4R^2-r^2}. \end{aligned} \tag{A.1}$$

Further with the cosine law $\cos\beta_1 = 1 - R^2/2r^2$ and $\cos\beta_2 = R/2r$, one gets the expression of $S$ as follows

$$S = \left[R^2 \ \arccos\left(1 - \frac{r^2}{2R^2}\right) + r^2 \ \arccos\left(\frac{r}{2R}\right)\right] - \frac{r}{2}\sqrt{4R^2 - r^2}. \tag{A.2}$$

As $S/L^2$ denotes the possibility that a specific agent is in this shaded region, the possibility that none of the $N-1$ agents is in this area equals $(1-S)^{N-1}$. Further considering the distance between agent $i$ and the GA, we arrive the possibility $f_{\text{th}}$ as follows

$$f_{\text{th}} = \int_{r_{\text{L}}}^{r_{\text{U}}} \left(1 - \frac{S}{L^2}\right)^{N-1} \cdot \frac{2\pi R}{L^2} \ \mathrm{d}R. \tag{A.3}$$

The lower limit of the integration $r_L = r$ since if GA is in the $r$-disk of agent $i$, the agent $i$ will directly connects the GA, and hence a connection is formed. To evaluate the upper limit $r_U$, we approximate the square plane $\Gamma$ as a circle area with the same area $L^2$, then $r_U$ is estimated as the radius of the circle area which gives $\pi r_U^2 = L^2$, i.e. $r_U = L/\sqrt{\pi}$. This approximation has a high accuracy when $L \gg r$. Applying the parameter values $N = 100$, $r = 0.1$, and $L = 1$ into equation (7), we obtain $f_{th} \approx 0.22$.

## ORCID iDs

Jie Zhou https://orcid.org/0000-0001-7006-2889
Yinzuo Zhou https://orcid.org/0000-0002-0997-3496

## References

[1] Boccaletti S, Kurths J, Osipov G, Valladares D L and Zhou C 2002 The synchronization of chaotic systems *Phys. Rep.* **366** 1
[2] Pikovsky A, Rosenblum M and Kurths J 2003 *Synchronization: A Universal Concept in Nonlinear Sciences* (Cambridge: Cambridge University Press)
[3] Arenas A, Díaz-Guilera A, Kurths J, Moreno Y and Zhou C 2008 Synchronization in complex networks *Phys. Rep.* **469** 93
[4] Dorogovtsev S N, Goltsev A V and Mendes J F F 2008 Critical phenomena in complex networks *Rev. Mod. Phys.* **80** 1275
[5] Motter A E, Myers S A, Anghel M and Nishikawa T 2013 Spontaneous synchrony in power-grid networks *Nat. Phys.* **9** 191
[6] Bullo F, Cortés J and Martínez S 2009 *Distributed Control of Robotic Networks* (Princeton, NJ: Princeton University Press)
[7] Buscarino A, Fortuna L and Frasca M 2006 Dynamical network interactions in distributed control of robots *Chaos* **16** 015116
[8] Bartsch R P, Schumann A Y, Kantelhardt J W, Penzel T and Ivanov P C 2012 Phase transitions in physiologic coupling *Proc. Natl Acad. Sci. USA* **109** 10181
[9] Bartsch R P, Liu K K L, Bashan A and Ivanov P C 2015 Network physiology: how organ systems dynamically interact *PLoS One* **10** e0142143
[10] Ivanov P C, Liu K K L and Bartsch R P 2016 Focus on the emerging new fields of network physiology and network medicine *New J. Phys.* **18** 100201
[11] Huang D 2004 Stabilizing near-nonhyperbolic chaotic systems with applications *Phys. Rev. Lett.* **93** 214101
[12] Flunkert V, Yanchuk S, Dahms T and Schöll E 2010 Synchronizing distant nodes: a universal classification of networks *Phys. Rev. Lett.* **105** 254101
[13] Schröder M, Mannattil M, Dutta D, Chakraborty S and Timme M 2015 Transient uncoupling induces synchronization *Phys. Rev. Lett.* **115** 054101
[14] Nishikawa T and Motter A E 2010 Network synchronization landscape reveals compensatory structures, quantization, and the positive effect of negative interactions *Proc. Natl Acad. Sci.* **107** 10342
[15] Albert R and Barabási A 2002 Statistical mechanics of complex networks *Rev. Mod. Phys.* **74** 47–97
[16] Pastor-Satorras R, Castellano C, Van M P and Vespignani A 2015 Epidemic processes in complex networks *Rev. Mod. Phys.* **87** 925
[17] Petter H and Jari S 2012 Temporal networks *Phys. Rep.* **519** 97–125
[18] Perra N, Gonçalves B, Pastor-Satorras R and Vespignani A 2012 Activity driven modeling of time varying networks *Sci. Rep.* **2** 469
[19] Valdano E, Fiorentin M R, Poletto C and Colizza V 2018 Epidemic threshold in continuous-time evolving networks *Phys. Rev. Lett.* **120** 068302
[20] Koher A, Lentz H, Gleeson J P and Hövel P 2019 Contact-based model for epidemic spreading on temporal networks *Phys. Rev.* X **9** 031017
[21] Zhou J, Zou Y, Guan S, Liu Z and Boccaletti S 2016 Synchronization in slowly switching networks of coupled oscillators *Sci. Rep.* **6** 35979
[22] Igor V B, Vladimir N B and Martin H 2004 Blinking model and synchronization in small-world networks with a time-varying coupling *Physica* D **195** 188–206
[23] Belykh I, Belykh V and Hasler M 2005 Synchronization in complex networks with blinking interactions *Int. Conf. Physics and Control* IEEE pp 86–91
[24] Skufca J D and Bollt E M 2004 Communication and synchronization in disconnected networks with dynamic topology: moving neighborhood networks *Math. BioSci. Eng.* **1** 347
[25] Porfiri M, Stilwell D, Erik M B and Skufca J 2006 Random talk: random walk and synchronizability in a moving neighborhood network *Physica* D **224** 102
[26] Porfiri M, Stilwell D, Bollt E M and Skufca J 2007 Stochastic synchronization over a moving neighborhood network *Proc. Am. Control Conf.* p 1413
[27] Peruani F, Nicola E M and Morelli L G 2010 Mobility induces global synchronization of oscillators in periodic extended systems *New J. Phys.* **12** 092029
[28] Frasca M, Buscarino A, Rizzo A, Fortuna L and Boccaletti S 2008 Synchronization of moving chaotic agents *Phys. Rev. Lett.* **100** 044102
[29] Fujiwara N, Kurths J and Díaz-Guilera A 2011 Synchronization in networks of mobile oscillators *Phys. Rev.* E **83** 025101
[30] Frasca M, Buscarino A, Rizzo A and Fortuna L 2012 Spatial pinning control *Phys. Rev. Lett.* **108** 204102
[31] Dariani R, Buscarino A, Fortuna L and Frasca M 2011 Pinning control in a system of mobile chaotic oscillators *AIP Conf. Proc.* **1389** 1023
[32] Klinglmayr J, Kirst C, Bettstetter C and Timme M 2012 Guaranteeing global synchronization in networks with stochastic interactions *New J. Phys.* **14** 073103
[33] Col L D, Tarbouriech S and Zaccarian L 2016 Global $H^\infty$ consensus of linear multi-agent systems with input saturation *Proc. Am. Control Conf.* p 6272
[34] Su H, Chen G, Wang X and Lin Z 2011 Adaptive second-order consensus of networked mobile agents with nonlinear dynamics *Automatica* **47** 368

[35] Hu W, Liu L and Feng G 2016 Consensus of linear multi-agent systems by distributed event-triggered strategy *IEEE Trans. Cybern.* **46** 148
[36] Qing H and Haddad W M 2008 Distributed nonlinear control algorithms for network consensus *Automatica* **44** 2375–81
[37] Wang X, Su H and Chen G 2017 Fully distributed event-triggered semiglobal consensus of multi-agent systems with input saturation *IEEE Trans. Ind. Electron.* **64** 5055
[38] Zhou J, Zou Y, Guan S, Liu Z, Xiao G and Boccaletti S 2017 Connection adaption for control of networked mobile chaotic agents *Sci. Rep.* **7** 16069
[39] Bartsch R P, Liu K K L, Ma Q D Y and Ivanov P C 2010 Three independent forms of cardio-respiratory coupling: transitions across sleep stages *Comput. Cardiol.* **41** 781 (PMID: 25664348)
[40] Bartsch R P and Ivanov P C 2014 Coexisting forms of coupling and phase-transitions in physiological networks *Commun. Comput. Info. Sci.* **438** 270
[41] Zhu X, Zhou J, Zou Y, Tang M and Xiao G 2019 Enhanced connection adaption strategy with partition approach *IEEE Access* **7** 34162
[42] Brock D, Hufnagel L and Geisel T 2006 The scaling laws of human travel *Nature* **439** 462
[43] Benhamou S 2007 How many animals really do the Lévy walk? *Ecology* **88** 1962
[44] Keeter M, Moore D, Muller R, Nieters E, Flenner J, Martonosi S, Bertozzi A, Percus A and Levy R 2012 Cooperative search with autonomous vehicles in a 3D aquatic testbed *Proc. Am. Control Conf.* p 3154
[45] Nishikawa T, Motter A E, Lai Y and Hoppensteadt F C 2003 Heterogeneity in oscillator networks: are smaller worlds easier to synchronize? *Phys. Rev. Lett.* **91** 014101
[46] Pecora L M and Carroll T L 1998 Master stability functions for synchronized coupled systems *Phys. Rev. Lett.* **80** 2109
[47] Xu L, Chen Z, Hu K, Stanley H E and Ivanov P C 2011 Spurious detection of phase synchronization in coupled nonlinear oscillators *Phys. Rev.* E **73** 065201
[48] Stilwell D, Bollt E M and Roberson G 2006 Synchronization of time-varying networks under fast switching *Proc. Am. Control Conf.* **5** 140
[49] Bashan A, Bartsch R P, Kantelhardt J W, Havlin S and Ivanov P C 2012 Network physiology reveals relations between network topology and physiological function *Nat. Commun.* **3** 702
[50] Ivanov P C and Bartsch R P 2014 *Network Physiology: Mapping Interactions Between Networks of Physiologic Networks* (Networks of Networks: The Last Frontier of Complexity) (Berlin: Springer ) ch 10